

Supporting Information for:

Understanding Ion Diffusion in Anion Exchange Membranes; Effects of Morphology and, Mobility of Pendant Cationic Groups

Mohammad Rezayani ^a, Farhad Sharif ^{a*}, Hesam Makki ^{b*}

^a Department of Polymer and Color Engineering, Amirkabir University of Technology, 424 Hafez Ave.,
Tehran, Iran.

^b Department of Chemistry and Materials Innovation Factory, University of Liverpool, Liverpool L69
7ZD, U.K.

Contents

1- DFT calculations.....	S1
1-1 Calculation method of partial charges.....	S1
1-2 System size analysis.....	S2
2- System compositions.....	S3
3- system equilibration.....	S4
3-1 Equilibration process for hydrated membranes.....	S4
3-2 Radius of gyration autocorrelation function.....	S4
4- Experimental and simulation density and diffusion coefficient data.....	S5
5- Radial distribution functions and coordination numbers.....	S5
6- Pore size distribution.....	S8
7- <i>MSD</i> of water	S8
8- Diffusion coefficient of methanol.....	S9
9- Subdiffusive behavior	S10
10- Calculation method of residence time	S11

1- DFT calculations

1-1 Calculation method of partial charges

Polymer chains contain 20 monomers (both functionalized and non-functionalized). For partial charge calculations, by using DFT, a tetramer with two neutral and two charged monomers in the center and the end has been assumed (see Figure S1). Monomers in the middle of a long (real) polymer chain are represented by the middle monomers of the tetramer. We have two types of monomers: charged (-1 e charge) and neutral (0 e charge). All partial charges of the tetramer's middle and end charged/neutral monomers are presented in Table S1.

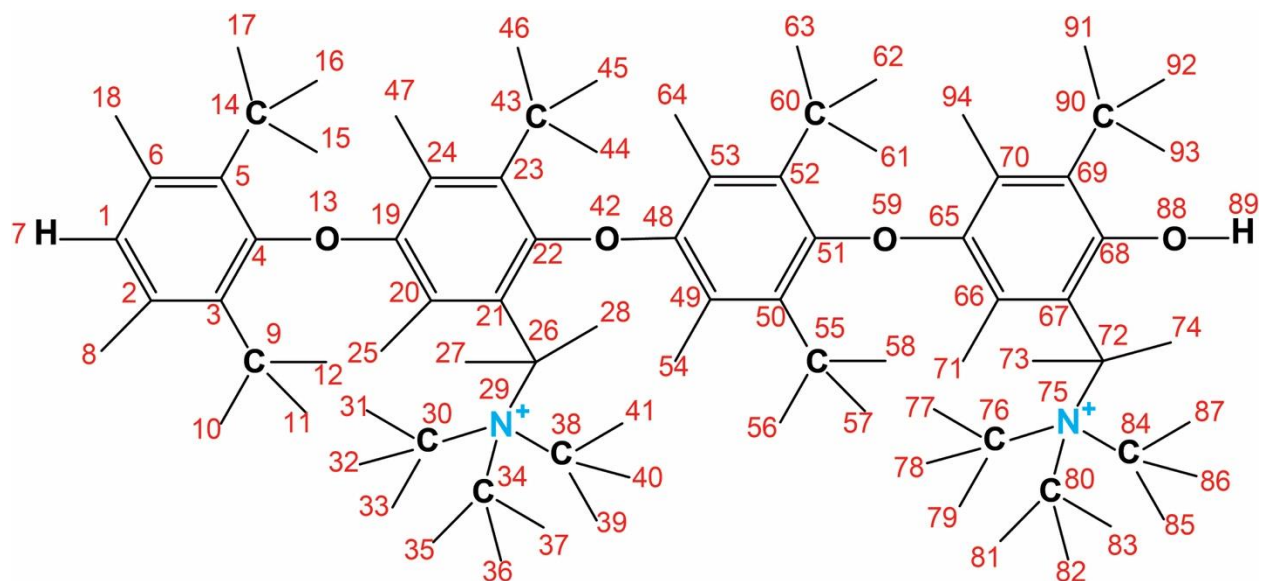


Figure S1. Schematic of a tetramer of an example structure for DFT calculation.

Table S1. Atomic partial charges for charged and neutral monomers as labeled in Fig S1.

Atom Number	Atom	Partial Charge	Atom Number	Atom	Partial Charge	Atom Number	Atom	Partial Charge
1	C	-0.022	33	H	0.168	65	C	0.233
2	C	-0.373	34	C	-0.402	66	C	-0.288
3	C	0.248	35	H	0.195	67	C	0.069
4	C	0.079	36	H	0.195	68	C	0.101
5	C	0.289	37	H	0.194	69	C	0.151
6	C	-0.387	38	C	-0.402	70	C	-0.266
7	H	0.148	39	H	0.193	71	H	0.163
8	H	0.197	40	H	0.189	72	C	-0.175
9	C	-0.304	41	H	0.198	73	H	0.169

10	H	0.059	42	O	-0.193	74	H	0.159
11	H	0.129	43	C	-0.422	75	N	0.090
12	H	0.107	44	H	0.139	76	C	-0.317
13	O	-0.336	45	H	0.148	77	H	0.170
14	C	-0.361	46	H	0.149	78	H	0.171
15	H	0.118	47	H	0.219	79	H	0.182
16	H	0.086	48	C	0.351	80	C	-0.356
17	H	0.129	49	C	-0.5097	81	H	0.211
18	H	0.194	50	C	0.320	82	H	0.211
19	C	0.458	51	C	-0.0597	83	H	0.201
20	C	-0.442	52	C	0.290	84	C	-0.449
21	C	0.369	53	C	-0.489	85	H	0.171
22	C	-0.242	54	H	0.2001	86	H	0.190
23	C	0.359	55	C	-0.3197	87	H	0.190
24	C	-0.432	56	H	0.080	88	O	-0.538
25	H	0.118	57	H	0.111	89	H	0.430
26	C	-0.372	58	H	0.111	90	C	-0.368
27	H	0.206	59	O	-0.269	91	H	0.141
28	H	0.178	60	C	-0.329	92	H	0.112
29	N	0.208	61	H	0.100	93	H	0.111
30	C	-0.314	62	H	0.091	94	H	0.131
31	H	0.179	63	H	0.120			
32	H	0.159	64	H	0.202			

1-2 System size analysis

The water anomalous diffusion coefficient, density, and *PLD* of different simulation box sizes contained 20, 30, 40, 50, and 60 chains were compared. As can be seen, the specified qualities are not influenced by the system size; therefore, we believe that the finite size effect is negligible for boxes containing above 20 polymer chains. Note that boxes with 40 polymer chains were used for all the results shown in the paper.

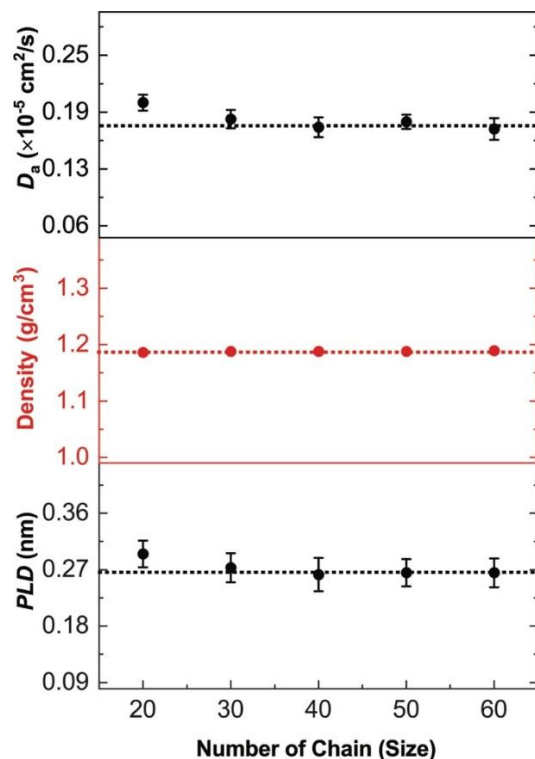


Figure S2. The anomalous diffusion coefficient (D_a), Density, and PLD parameters for different system sizes of PPO-BTMA at $\lambda = 5$.

2- System compositions

Table S2 shows the polymer chain, water, and anion composition of each simulation box. Note that, λ is the number of water molecules per cationic group.

Table S2. Number of polymer chains, anion, and hydration level for each simulation box

Sample	Number of polymer chains	λ	Number of water molecules	Number of Br^-
PPO-BTMA	40	2-15	640-4800	320
PPO-QC6	40	2-15	640-4800	320
PPO-QC10	40	2-15	640-4800	320
PPO-QC16	40	2-15	640-4800	320
PPO-C8QC8	40	2-15	640-4800	320
PPO-C16Q	40	2-15	640-4800	320

3- System equilibration

3-1 Equilibration process for hydrated membranes

For the equilibration process, we, initially, selected membranes with the maximum degree of hydration ($\lambda = 15$) and then put them under the minimization process by using the steepest descent algorithm to minimize the potential energy of the system. After that, a 5 ns simulation was performed (in NPT) to achieve a compressed box with a constant density. In the next step, the annealing procedure was applied to the simulation boxes, during which the temperature of the simulation box rose to 1000K in a period of 10 ns allowing the hydrated membrane for further relaxation. Once the box temperature reached the defined temperature, the box cooled down to 295 K in a four-step process (200 K each step and 105 K for the last step over 3 ns for each step). In the next stage, annealed simulation box underwent another 5 ns MD simulation (in NPT) again to maintain constant pressure and temperature. A Time step of 1 fs was chosen for all relaxation procedures. After the equilibration process, a production run of 100 ns with a time step of 2 fs was conducted (in NPT).

3-2 Radius of the gyration autocorrelation function

The squared radius of gyration autocorrelation function is presented in Fig S3 for randomly selected membranes at $\lambda = 15$, with the dotted line serving as a visual cue to the zero point. The squared radius of gyration autocorrelation function of all samples converges before 13 ns, indicating that the simulation time (100 ns) is long enough to result in equilibrated membranes. The calculations were carried out up to 100 ns, however, only the results up to 50 ns are reported because the ACF oscillations after 50 ns.

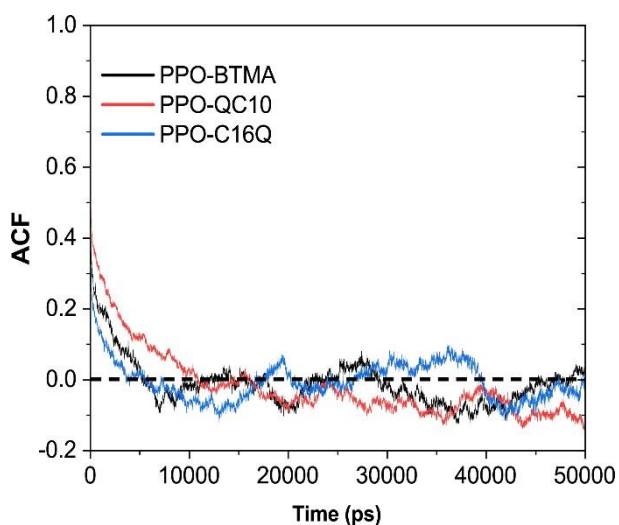


Figure S3. Autocorrelation function of the squared radius of gyration at $\lambda = 15$ for different membranes.

4- Experimental and simulation density and diffusion coefficient data

To be confident that the selected force field and method of simulation reproduce the main features of our membranes, we calculated the density of dried membranes and simulation diffusion coefficient data of hydrated membranes and compared those with the experimental ones from the work of Thieu et al ¹. Table S3 compares the density data of the simulations with the corresponding experimental ones.

Table S3. Sample densities of simulation end experiment¹

Sample	Density (Experimental) g/cm ³	Density (Simulation) g/cm ³	% Error
PPO-BTMA	1.25	1.19	4.8
PPO-QC6	1.15	1.11	3.47
PPO-QC10	1.13	1.07	5.31
PPO-QC16	1.12	1.052	6.07

Figure S4 demonstrates the self-diffusion data of experiments and anomalous diffusion coefficient of simulations for PPO-QA membranes. As shown, simulation data follow a very similar trend compared to experiment diffusion data.

Table S4. Self-diffusion coefficient of PPO-QA with different side-chain lengths, experiment, and simulation. Note that $D \propto (10^{-5} \text{ cm}^2/\text{s})$.

AEM-BTMA															
Experiment		Simulation													
$\lambda(\approx)$	$D(\approx)$	λ	D_a												
5.2	0.19	2	0.099	3.75	0.03	2	0.0218	3.8	0.01	2	0.0122	3.2	0.01	2	0.0179
6.5	0.23	4	0.1479	3.85	0.04	4	0.0401	4	0.01	4	0.0122	3.3	0.015	4	0.0309
7.3	0.24	5	0.1823	5.3	0.06	5	0.052	5.2	0.02	5	0.016	4.5	0.02	5	0.0255
8	0.28	6	0.1967	5.7	0.075	6	0.083	6.2	0.03	6	0.0503	8	0.045	6	0.0244
		8	0.2615			8	0.1583			8	0.13			8	0.059
		10	0.3973			10	0.2722			10	0.2234			10	0.12061
		12	0.523			12	0.3869			12	0.3684			12	0.22038
		14	0.665			14	0.4961			14	0.4969			14	0.3192
		15	0.71			15	0.5236			15	0.5138			15	0.4711

5- Radial distribution functions and coordination numbers

Radial distribution functions and coordination numbers of Nitrogen-Nitrogen (QA groups), Nitrogen-Oxygen (water), Oxygen (water)-Oxygen (Water), Nitrogen (QA)- Br⁻ at different hydration levels for PPO-QA membranes with different extender length ($n = 0, 6, 10, 16$) are presented in Figure S5. As shown, $g_{N-N}(r)$ of all membranes decrease in high and move to longer distance due to the density of water molecules surrounding QA groups and push them to

farther distances. On the other hand, $g_{N-O_w}(r)$ peaks of the membranes show a decreasing behavior as a result of the solvation effect. The internal structure of water molecules is analyzed using $g_{O_w-O_w}(r)$ to study the three-dimensional structure of the water phase. It is concluded that water molecules are surrounded by more water molecules as hydration increases and the internal structure of water is more packed. Finally, $g_{N-Br}(r)$ peak height decreases with an increase in hydration, indicating that water molecules surround cationic groups and push anions to longer distances and decrease the accessibility of anions to cationic groups.

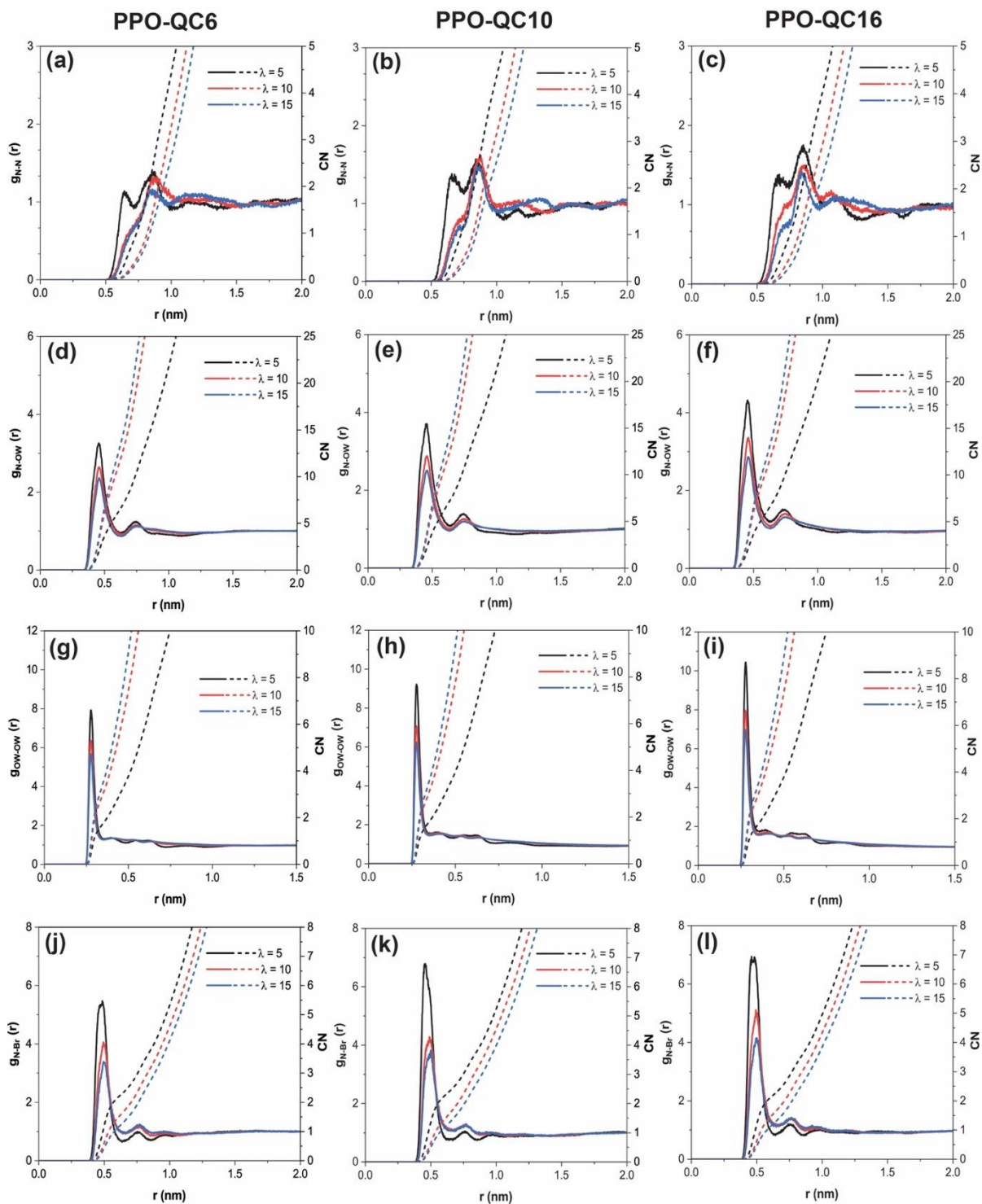


Figure S4. (a), (b), (c) $g_{N-N}(r)$ and CN, (d), (e), (f) $g_{N-ow}(r)$ and CN, (g), (h), (i) $g_{ow-ow}(r)$ and CN for, (j), (k), (l) $g_{N-Br}(r)$ and CN for different membranes at various hydration levels.

6- Pore size distribution

Figure S6 represents the *PSD* of membranes at various hydration levels. It is evident that all samples show a high peak at around 0.36 nm which shifts to right at higher hydration levels.

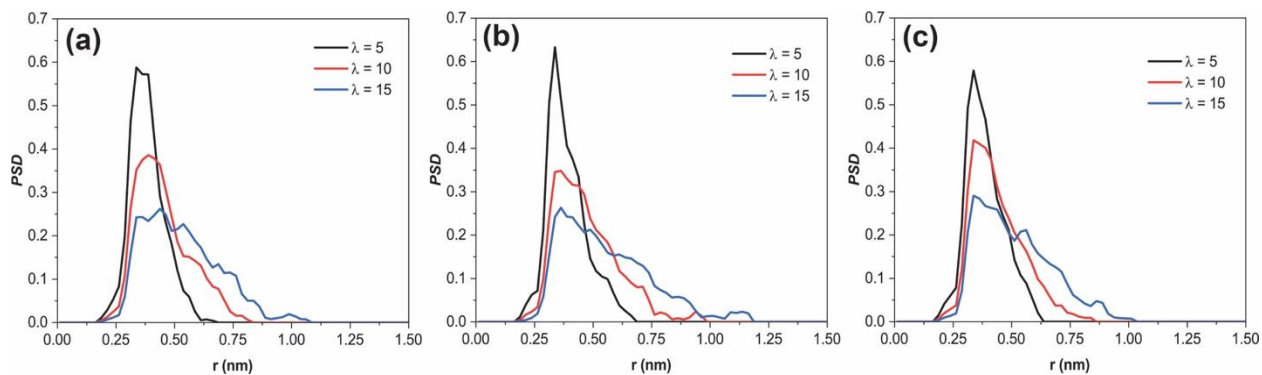


Figure S5. Pore size distribution (PSD) of (a) PPO-QC6 and (b) PPO-QC10 and (c) PPO-QC16 membranes at different hydration levels.

7- MSD of water

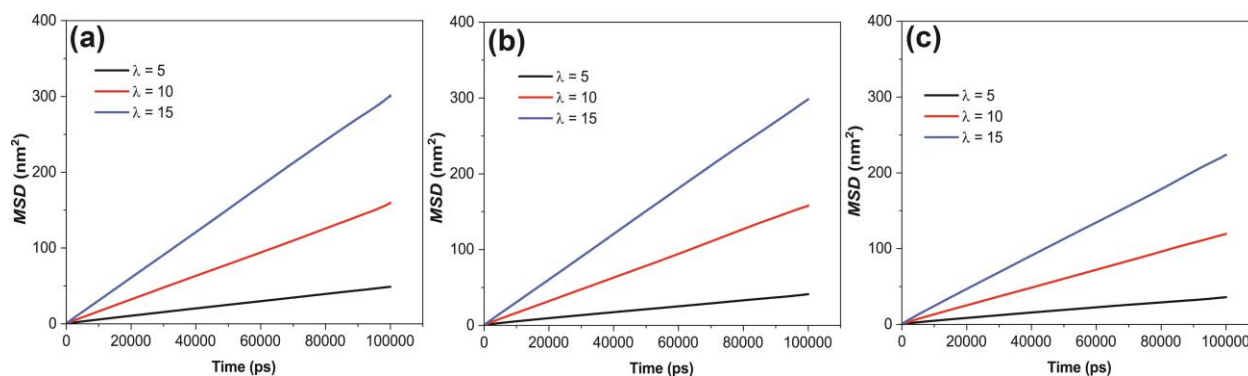


Figure S6. MSD of (a) PPO-QC6 and (b) PPO-QC10 and (c) PPO-QC16 membranes at different hydration levels.

8- Diffusion coefficient of methanol

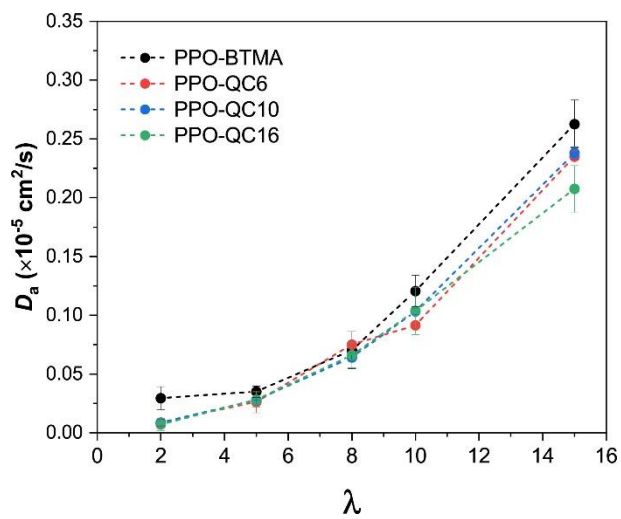


Figure S7. Diffusion coefficient (D_a) of methanol as a function of λ

9- Subdiffusive behavior

The diffusive behavior of all samples at different hydration levels is shown in Fig S8. As shown, different membranes show different diffusive behavior under different conditions. All samples show a subdiffusive behavior very far from normal diffusion at $\lambda = 5$, while diffusion behavior is closer to the normal regime at $\lambda = 15$ for all membranes.

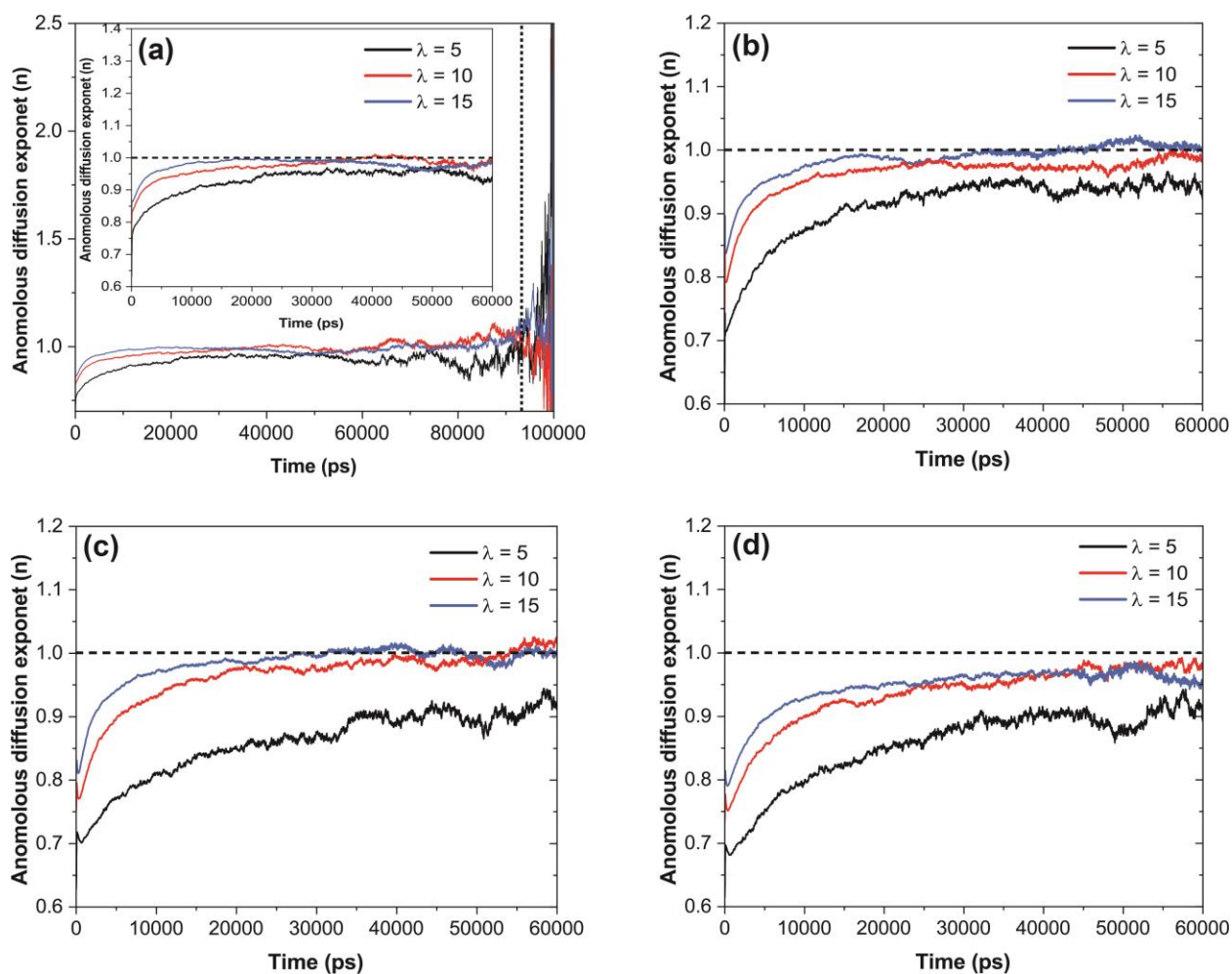


Figure S8. Subdiffusive exponent as a function of time for (a) PPO-QC6, (b) PPO-QC10 (c) PPO-QC16

10- Calculation method of residence lifetime

Residence time autocorrelation function ($C_{res}(t)$) is shown as ^{2,3}.

$$C_{res}(t) = \frac{\langle g(0)g(t) \rangle}{\langle g(0)^2 \rangle}$$

where $g(t) = 1$ if the water molecule is within the first hydration shell and $g(t) = 0$ if the water molecule is outside the shell. To obtain residence time, the calculated residence time autocorrelation function of water is fitted with a three exponential function which gives more reliable results³.

$$C_{res}(t) = a_1 \exp(-t/\tau_1) + a_2 \exp(-t/\tau_2) + a_3 \exp(-t/\tau_3)$$

where $a_3 = 1 - a_2 - a_1$ and τ_3 is the residence time of the water molecule in the first hydration shell.

References

- (1) Thieu, L. M.; Zhu, L.; Korovich, A. G.; Hickner, M. A.; Madsen, L. A. Multiscale Tortuous Diffusion in Anion and Cation Exchange Membranes. *Macromolecules* **2018**, *52* (1), 24–35.
- (2) Reddy, T. D. N.; Mallik, B. S. Heterogeneity in the Microstructure and Dynamics of Tetraalkylammonium Hydroxide Ionic Liquids: Insight from Classical Molecular Dynamics Simulations and Voronoi Tessellation Analysis. *Physical Chemistry Chemical Physics* **2020**, *22* (6), 3466–3480.
- (3) Skarmoutsos, I.; Welton, T.; Hunt, P. A. The Importance of Timescale for Hydrogen Bonding in Imidazolium Chloride Ionic Liquids. *Physical Chemistry Chemical Physics* **2014**, *16* (8), 3675–3685.